SCIENTIFIC REPORTS

OPEN

SUBJECT AREAS:
BIOMATERIALS - PROTEINS
BIOMEDICAL MATERIALS
REGENERATIVE MEDICINE
TISSUE ENGINEERING

Received
8 October 2012

Accepted
2 November 2012

Published
6 December 2012

Correspondence and requests for materials should be addressed to H.M. (hmori@kit.ac.jp)

* These authors contributed equally.

Bone regeneration by polyhedral microcrystals from silkworm virus

Goichi Matsumoto[1]*, Takayo Ueda[2], Junko Shimoyama[1], Hiroshi Ijiri[2], Yasushi Omi[1], Hisato Yube[1], Yoshihiko Sugita[3], Katsutoshi Kubo[3], Hatsuhiko Maeda[3], Yukihiko Kinoshita[3], Duverney Gaviria Arias[4], Junji Shimabukuro[2], Eiji Kotani[2], Shin Kawamata[5] & Hajime Mori[2,6]*

[1]Department of Oral and Maxillofacial Surgery, Kanagawa Dental College, 82 Inaoka, Yokosuka, Kanagawa 238-8580, Japan, [2]Insect Biomedical Research Center, Kyoto Institute of Technology, Matsugasaki, Sakyo-ku, Kyoto 606-8585, Japan, [3]Department of Oral Pathology, School of Dentistry, Aichi-Gakuin University, 1-100 Kusumoto-cho, Chikusa-ku, Nagoya 464-8650, Japan, [4]Centre for Molecular Biology and Biotechnology Health Sciences, Faculty-Universidad Tecnologica de Pereira, Pereira, Colombia, [5]Basic Research Group for Regenerative Medicine, Foundation for Biomedical Research and Innovation, TR1308, 1-5-4 Minatojima-minamimachi, Kobe 650-0043, Japan, [6]Protein Crystal Corporation, 1-12-8 Senba Higashi, Minoh 541-0053, Japan.

***Bombyx mori* cypovirus is a major pathogen which causes significant losses in silkworm cocoon harvests because the virus particles are embedded in micrometer-sized protein crystals called polyhedra and can remain infectious in harsh environmental conditions for years. But the remarkable stability of polyhedra can be applied on slow-release carriers of cytokines for tissue engineering. Here we show the complete healing in critical-sized bone defects by bone morphogenetic protein-2 (BMP-2) encapsulated polyhedra. Although absorbable collagen sponge (ACS) safely and effectively delivers recombinant human BMP-2 (rhBMP-2) into healing tissue, the current therapeutic regimens release rhBMP-2 at an initially high rate after which the rate declines rapidly. ACS impregnated with BMP-2 polyhedra had enough osteogenic activity to promote complete healing in critical-sized bone defects, but ACS with a high dose of rhBMP-2 showed incomplete bone healing, indicating that polyhedral microcrystals containing BMP-2 promise to advance the state of the art of bone healing.**

Most secreted molecules including growth factors, chemokines and cytokines do not diffuse far but are bound to the cell surface or surrounding extracellular matrices (ECM) to regulate cell function *in vivo*. The ECM functions as a reservoir for various kinds of soluble growth factors. Indeed, ECM-bound growth factors are released from the ECM after proteolytic cleavage to alter cell behavior. Conversely, cells regulate degradation or remodeling of the ECM by secreting proteases and their inhibitors. Thus, the behavior of individual cells and tissue dynamics are regulated by intricate reciprocal interactions between cells and their surrounding micro-environment. Considering a dynamic complexity of the *in vivo* situation, there is an urgent need to develop new tools to reconstitute or modulate the extracellular micro-environment *in vitro*.

Bone morphogenetic proteins, members of the transforming growth factor-β (TGF-β) superfamily, are disulfide-linked homodimers that induce bone and cartilage formation. Research has shown that BMP-2 induces new bone formation in animal models. It is now well recognized to be one of the key osteogenic factors in the field of bone-tissue engineering[1–3], and it has been approved for limited clinical use in the form of rhBMP-2[4].

For the best healing, rhBMP-2 should be present in the healing tissue at a constant concentration. Although an external metering system that delivers the drug continuously into the healing tissue through a tube is theoretically possible, large practical hurdles stand in the way of implementing such a system. A more attractive alternative, in our opinion, is to implant a carrier or reservoir that contains a dose of rhBMP-2 sufficient to promote healing over several weeks but that releases the drug slowly and continuously into the site of healing bone. Biocompatible, biodegradable, non-toxic, and immunologically inert materials are available, and some of them have already been approved for clinical use as a carrier for rhBMP-2. However, none of them, including ACS, release rhBMP-2 slowly and steadily. They all release the growth factor too quickly at the beginning of therapy[5].

Although ACS can physically adsorb rhBMP-2, BMP-2 does not bind to its fibers sufficiently[6,7]. Its release, governed by factors other than degradation of the ACS, is therefore unpredictable *in vivo*. In addition to the problem of unpredictable release, the half-life of rhBMP-2 *in vivo* is short; it is rapidly degraded[8]. Consequently, milligram doses are necessary in order for protein-based therapies to achieve the desired osteogenic results[4,9,10]. Not only is such high-dose therapy prohibitively expensive for normal clinical use, but there are also concerns that

high doses of rhBMP-2 cause cancer[9,11–13]. Although researchers have tested a number of natural and synthetic biomaterials as delivery systems that control the release of rhBMP-2[14], a satisfactory solution to this problem is not yet in hand. Here we report our experiments with a novel genetically engineered biomaterial that contains sequestered BMP-2 and that releases the growth factor slowly into a healing site. The material that we describe is derived from the naturally occurring protein called polyhedrin.

Several insect viruses produce polyhedra as a part of their reproductive cycle. These viruses produce polyhedrin protein and progeny virus particles such that the progeny particles are occluded into polyhedra and are thereby protected from a potentially hostile environment[15–17]. These polyhedra are the main vectors that transport the particles of this family of viruses from one insect host to another. Under physiological conditions, polyhedra are inert and their solubility is low. They resist attack by detergents and other corrosive materials[17]. Despite this resistance, they will release substances sequestered within them slowly as a result of the degradation caused by proteases secreted from surrounding cells *in vivo*. By virtue of their structural and chemical characteristics, these insect-virus polyhedral microcrystals are capable of slowly and continuously delivering a therapeutic drug into a wound. Such is the inspiration for the present set of experiments.

The *Bombyx mori* cypovirus (BmCPV) is one of the viruses that produce polyhedra in which many progeny virus particles are occluded. With genetic engineering, we have successfully produced recombinant polyhedral microcrystals made with polyhedrin protein derived from the BmCPV[18,19]. Thus, these genetically engineered polyhedra contain no progeny virus particles; we call them 'sterile' polyhedra. In a further step, we developed a technique by which to incorporate BMP-2 into the sterile polyhedra.

Results

Construction of BMP-2 polyhedra. BMP-2 exists as several forms: BMP-2 is expressed as a precursor of 396 amino acids (full-length BMP-2), the pro-form of BMP-2 (pro BMP-2) has no signal peptide, while mature BMP-2 is processed from the pro-form of BMP-2 (Fig. 1A). In this study, full-length, pro-form and mature BMP-2 were fused with VP3 or H1 tags[19] and immobilized in BmCPV polyhedra (Fig. 1B). Mature BMP-2 was fused with VP3-S at the C-terminus, or VP3-L and H1 at the N-terminus. Pro BMP-2 was fused with VP3-S, -L, and H1 at the N-terminus. Full-length BMP-2 was fused with VP3-S at the C-terminus, or VP3-S, -L, and H1 at the N-terminus. As BMP-2 is known to act as a disulfide-linked homodimer and induces bone regeneration, BMP-2 polyhedra were produced using recombinant baculovirus expressing BmCPV polyhedrin and protein disulfide bond isomerase (PDI). The immobilization of each form of BMP-2 into polyhedra was confirmed by performing SDS-PAGE and western blot analysis (Supplementary Fig. S1).

Chondrogenic and osteogenic differentiation of ATDC5 cells by BMP-2 polyhedra. To evaluate whether BMP-2 polyhedra acted as a biologically active substance to enhance bone regeneration, we analyzed the effects of BMP-2 polyhedra on chondrogenic differentiation and phosphorylation of Smad1/5 in the ATDC5 cell line. ATDC5 cells are a suitable cell line for investigation of chondrogenic and osteogenic differentiation because early phases in culture display cartilage differentiation and late phases undergo bone differentiation.

A 24-well plate was spotted with desiccated BMP-2 polyhedra or empty polyhedra (CP-H polyhedra) and ATDC5 cells were seeded on and around the polyhedron spot. Early phase differentiation of cartilage nodule formation was examined for the amount of sulfated glycosaminoglycan by alcian blue staining. Polyhedra containing full-length BMP-2 with VP3-S and H1 tags at the N-terminus promoted chondrogenic differentiation compared with the other BMP-2

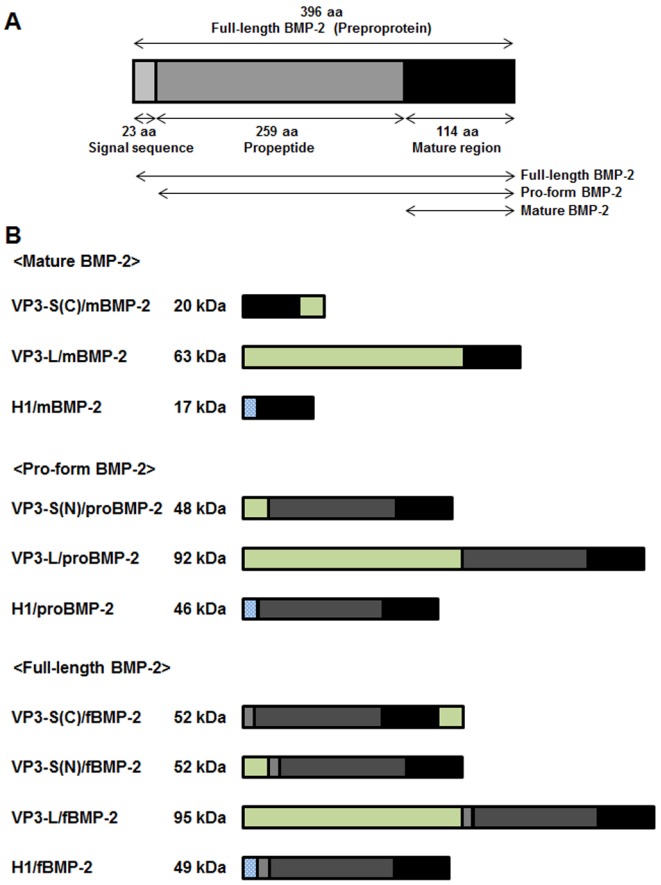

Figure 1 | Structures of BMP-2 for encapsulation into BmCPV polyhedra. (A) Full-length BMP-2 (396 aa) is consisted of signal sequence (23 aa), propeptide (259 aa), and mature region (114 aa). (B) Full-length, pro-form and mature BMP-2 were fused with VP3 or H1 tags to be immobilized into BmCPV polyhedra.

polyhedra and CP-H polyhedra (Fig. 2A, B). During late phase osteogenic differentiation of ATDC5 cells, ECM is mineralized and exhibits characteristics similar to bone formation, which can be measured by alizarin red staining. Alizarin red staining was detected by ATDC5 cells cultivated with polyhedra containing pro BMP-2 with VP3-S and H1 at the N-terminus and full-length BMP-2 with VP3-S and H1 at the N-terminus, but the latter showed the most induction of osteogenic differentiation (Fig. 2C, D). After the growth and expansion of the nodules, hypertrophic chondrocytes appear in association with elevation of alkaline phosphatase (ALPase) activity, followed by matrix mineralization. The elevation of ALPase activity of ATDC5 cells was strongly induced by polyhedra containing full-length BMP-2 with the H1 tag (Supplementary Fig. S2). We concluded that polyhedra containing full-length BMP-2 with the H1 tag (H1/fBMP-2 polyhedra) had a similar biological activity to BMP-2.

BMPs are members of the TGF-β superfamily and members of the Smad family of signal transduction molecules are components of a critical intracellular pathway that transmit TGF-β signals from the cell surface into the nucleus. Smad1/5 transmits BMP-2 signaling and forms a complex with Smad4 to allow translocation to the nucleus for gene regulation of bone-specific differentiation. To investigate the activation of the TGF-β and BMP signaling pathways, the phosphorylation of Smad1/5 in ATDC5 cells was examined using a phospho-Smad1/5 monoclonal antibody. Phosphorylation of Smad1/5 protein was observed after 1 hr in ATDC5 cells incubated with H1/fBMP-2 polyhedra and was maintained for 24 hrs. In contrast, these phosphorylation events were not evident in ATDC5 cells incubated with empty polyhedra (CP-H polyhedra) (Fig. 3A).

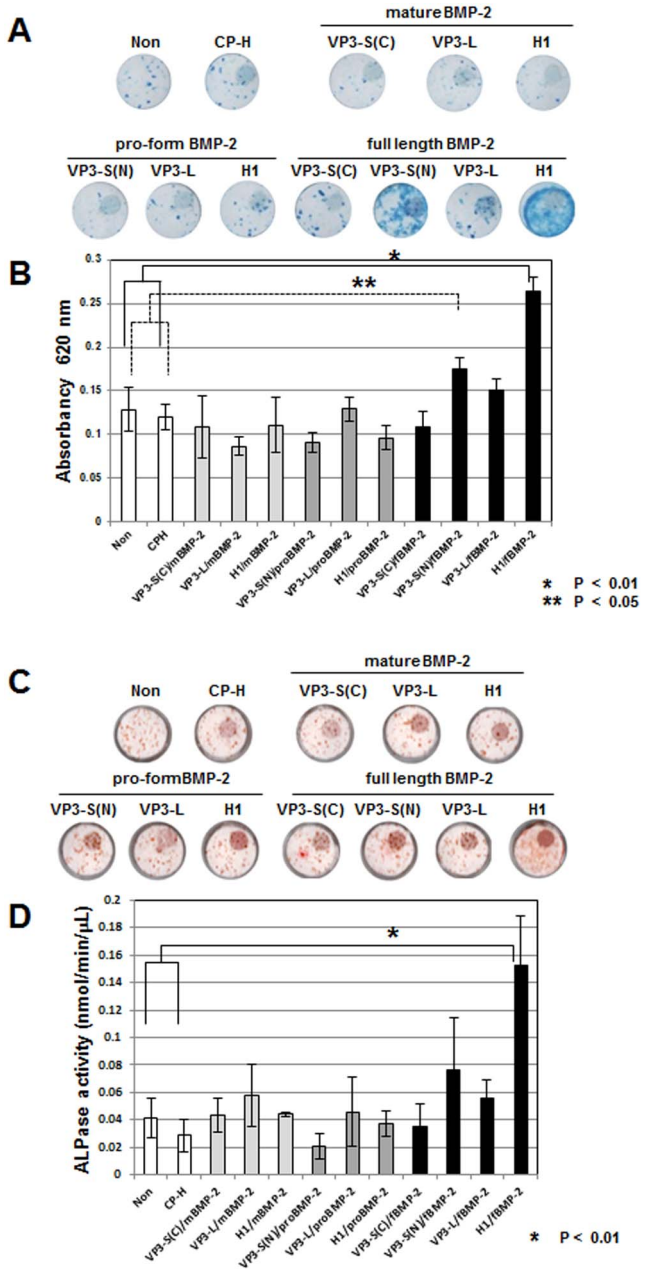

Figure 2 | Chondrogenic and osteogenic differentiation of ATDC5 cell by BMP-2 polyhedra. BMP-2 polyhedra or CP-H polyhedra were spotted and ATDC5 cells were seeded on and around polyhedron spot. Early phase differentiation of cartilage nodule formation was examined with an amount of glycosaminoglycan by alcian blue staining (A and B). At late phase osteogenic differentiation of ATDC5, mineralization of extracellular matrix is measured by arizarin red staining (C and D).

Estimation of activity of H1/fBMP-2 polyhedra and assay of release of BMP-2 from H1/fBMP-2 polyhedra. BMP-2 activity of H1/fBMP-2 polyhedra was quantified by the amount of alcian blue staining of sulfated glycosaminoglycan, which shows the early differentiation phase of cartilage formation by ATDC5 cells, compared to the soluble form of recombinant human BMP-2 (rhBMP-2). Absorbance at 620 nm was increased by BMP-2 in a dose-dependent manner. The maximum absorbance attained was at a dose of 31 ng/ml and alcian blue staining was inhibited by larger doses of rhBMP-2. BMP-2 activity from 3.6×10^7 H1/fBMP-2 polyhedra was estimated to be equivalent to the activity of 1 μg rhBMP-2 (Fig. 3B).

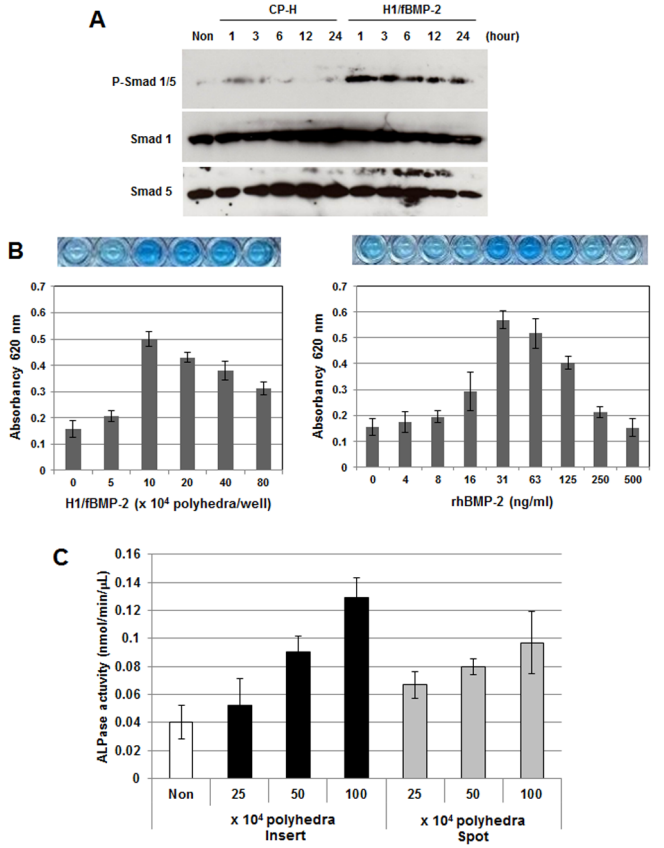

Figure 3 | Phosphorylation of Smad family by H1/fBMP-2 polyhedra and estimation of activity of H1/fBMP-2 polyhedra. (A) ATDC5 cells were co-incubated with H1/fBMP-2 polyhedra and empty polyhedra (CP-H polyhedra). Phosphorylation of Smad1/5 of ATDC5 cells was assayed by use of phospho-Smad1/5 monoclonal antibody. (B) Activity of BMP-2 from H1/fBMP-2 polyhedra were estimated by comparison with that of rhBMP-2. This activity was quantified by the amount of alcian blue staining of glycosaminoglycan which shows early phase differentiation of cartilage formation of ATDC5 cells. (C) Release of BMP-2 from H1/fBMP-2 polyhedra. H1/fBMP-2 polyhedra were spotted on the membrane of cell culture inserts and ATDC5 cells were seeded in each well of the cell culture plate. The late phase osteogenic differentiation of ATDC5 cells was assayed by ALPase activity.

H1/fBMP-2 polyhedra were spotted on the membrane of cell culture inserts and ATDC5 cells were seeded in each well of the cell culture plate. The late phase osteogenic differentiation of ATDC5 cells was assayed by ALPase activity. ALPase activity was dependent on the number of H1/fBMP-2 polyhedra in the cell culture insert and increased with dose. Osteogenic differentiation was more highly enhanced by H1/fBMP-2 polyhedra in the cell culture insert rather than H1/fBMP-2 polyhedra in proximity to cells. This indicated that BMP-2 is more efficiently released from H1/fBMP-2 polyhedra (Fig. 3C).

Surgical procedure for assay of bone regeneration. Numbers of 1.8×10^7 or 3.6×10^6 of H1/fBMP-2 polyhedra and empty polyhedra (CP-H polyhedra) were suspended with 50 μl PBS and incorporated into an ACS. A 50 μl aliquot of rhBMP-2 solution prepared with 5 μg or 1 μg in PBS was dropped onto the sponge to make the rhBMP-2 ACS. We prepared a 9 mm-diameter bone defect in the calvaria bone with a trephine bur copiously irrigated with sterile saline water. Rats were divided into seven experimental groups consisting of 12 rats in each group. Groups 1 to 6 were treated with 1.8×10^7 H1/fBMP-2 polyhedra, 3.6×10^6 H1/fBMP-2

polyhedra, 5 μg of rhBMP-2, 1 μg of rhBMP-2, 1.8×10^7 CP-H polyhedra, 3.6×10^6 CP-H polyhedra and group 7 was treated without implant. The rats in each group were further divided into three groups (4 rats/group) depending on the duration of the experiment (5, 10 and 15 weeks). ACS was placed in the bone defects of each rat in experimental groups 1 to 6. (Fig. 4).

Osteoinductive effects of H1/fBMP-2. X-ray radiographs of the calvaria bone defects at 5, 10, and 15 weeks after implantation showed the state of bone regeneration. At 5 weeks, radiopaque regions are clearly visible at the bone-defect sites where ACS containing sequestered H1/fBMP-2 polyhedra had been implanted. In contrast, radiopaque regions were not visible in the other experimental groups. At 10 and 15 weeks after implantation, the size of the radiopaque regions clearly showed that the largest amount of bone had formed at the bone-defect sites in which ACS containing H1/fBMP-2 polyhedra was implanted (Fig. 5A). Radiographic analysis revealed that little or no bone regeneration took place in the rhBMP-2, CP-H polyhedra, and control groups during the 15-week period of this study. The bone mineral content (BMC) of tissue also clearly showed that more bone formed at bone-defect sites that received implants of ACS with sequestered H1/fBMP-2 polyhedra than had formed at bone-defect sites in the rats in the other groups (Fig. 5B).

To evaluate the extent of bone regeneration after implantation, the calvaria bone specimens were harvested for μ-CT scanning and 3-D images were reconstructed. There was almost no regenerated bone in the bone defects in the rhBMP-2, empty polyhedron, and control groups except in the immediate vicinity of the bone-defect margins. This demonstrates that sequestered rhBMP-2 in ACS induced only a small amount of new bone regeneration. In contrast, when H1/fBMP-2 polyhedra was sequestered in ACS, significant regeneration took place. At 15 weeks after implantation, μ-CT images indicated healing in two of the four defects that had received 3.6×10^6 H1/fBMP-2 polyhedra. The other two defects demonstrated some bone regeneration but had not healed completely. In contrast, all bone defects implanted with ACS containing 1.8×10^7 H1/fBMP-2 polyhedra were completely healed (Fig. 6A).

To quantify newly generated bone, we evaluated bone volume (BV) at 15 weeks after implantation by μ-CT scanning. Compared with the control group, the rhBMP-2 group had increased BV, but there was no significant difference between these two groups. In contrast, H1/fBMP-2 polyhedra significantly improved BV

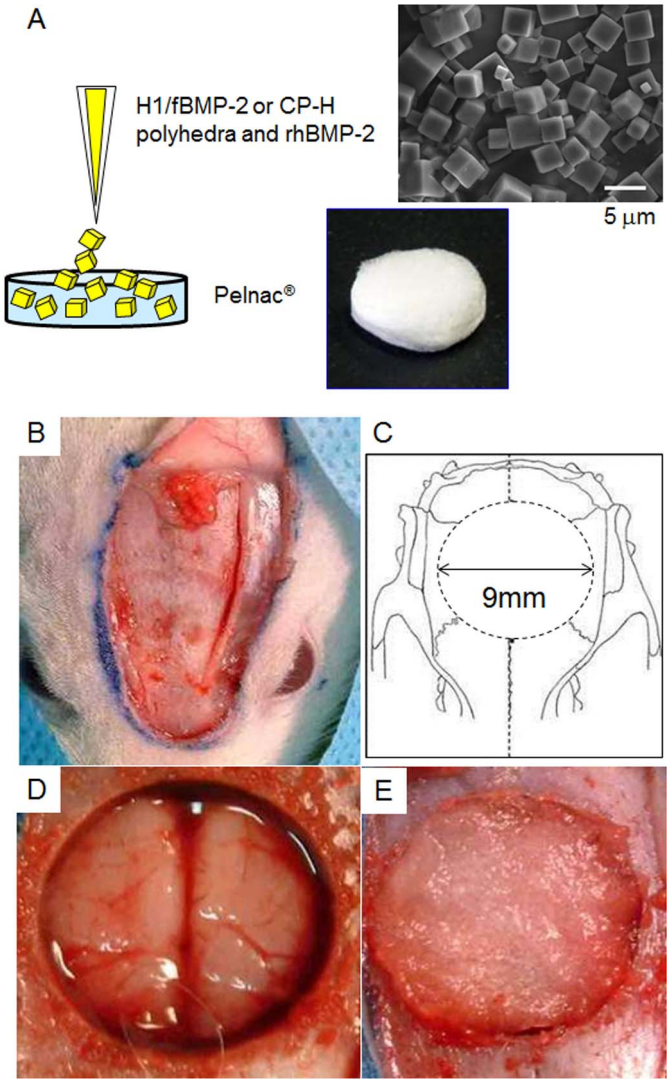

Figure 4 | Surgical procedure for *in vivo* bone regeneration. (A) H1/fBMP-2 polyhedra, CP-H polyhedra, and rhBMP-2 was dropped onto ACS. (B) The skin and underlying tissues including periosteum were reflected to expose the calvarial bone. (C, D) Critical-sized defect (9 mm in diameter) was created on the calvarial bone. (E) An ACS was implanted into the bone defect.

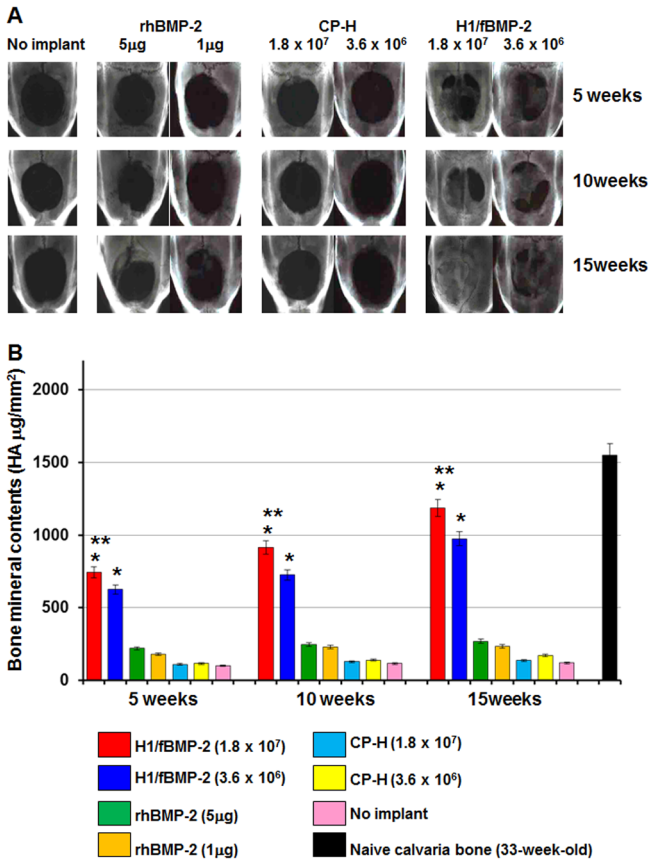

Figure 5 | Radiographic appearance of calvarial bone defects after application with no implant (No implant), ACS with rhBMP-2 (rhBMP-2), ACS with empty polyhedra (CP-H), and ACS with H1/fBMP-2 polyhedra (H1/fBMP-2). (A) Sequential radiographic photos show bone regeneration at 5, 10, and 15 weeks after implantation in the experimental group. (B) BMC in calvarial bone defects after implantation. BMC is shown at 5, 10, and 15 weeks after implantation. * indicates significantly different from rhBMP-2, CP-H polyhedron, and no implant group ($p<0.01$). ** indicates significantly different from H1/fBMP-2 polyhedron group with 3.6×10^6 polyhedral microcrystals ($p<0.05$).

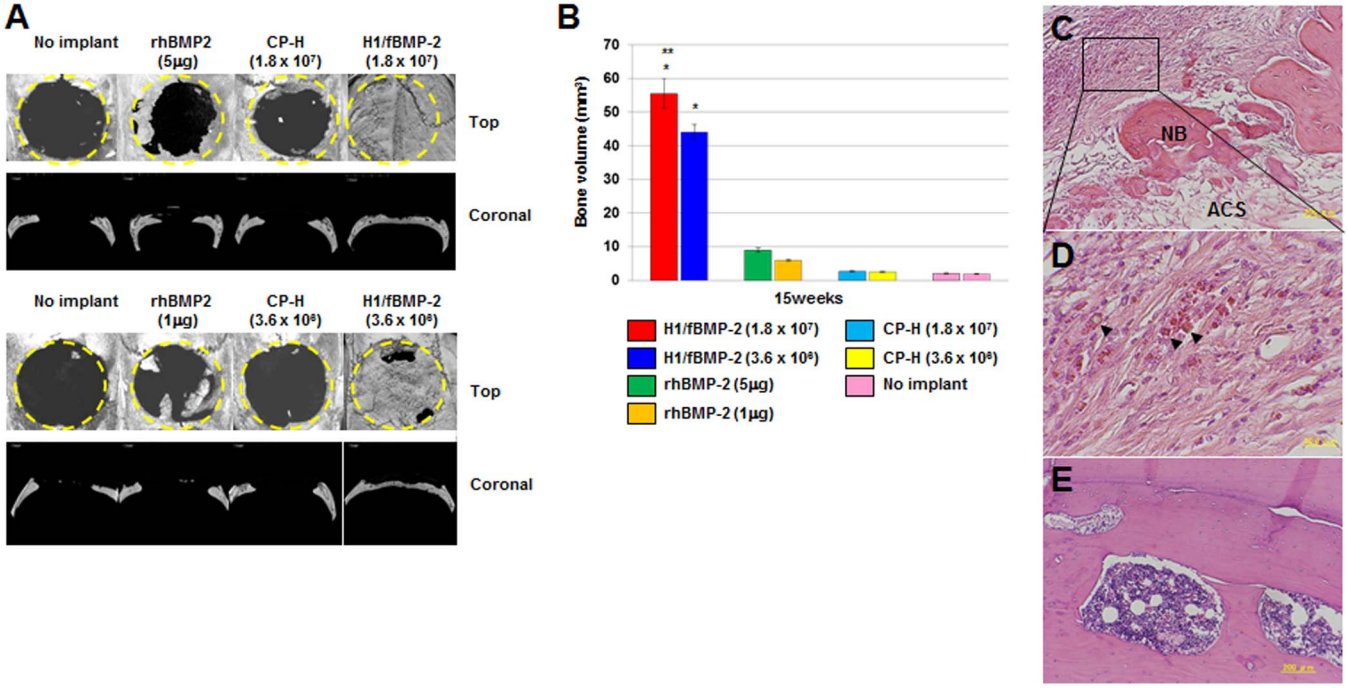

Figure 6 | Bone formation in critical-sized calvarial defect 15 weeks after implantation. (A) The μ-CT analysis was performed to visualize and quantify bone regeneration. The 3-D images were reconstructed to illustrate the top and coronal section views of no implant (No implant), ACS with rhBMP-2 (rhBMP-2), ACS with empty polyhedra (CP-H), and ACS with H1/fBMP-2 polyhedra (H1/fBMP-2). The dotted line represents the surgical margin of the calvaria bone defect. (B) Newly generated bone was evaluated by bone volume in bone defects assessed from the projected area of the μ-CT images. * indicates significantly different from rhBMP-2, CP-H polyhedron, and no implant group ($p<0.01$). ** indicates significantly different from H1/fBMP-2 polyhedron group with 3.6×10^6 polyhedral microcrystals ($p<0.05$). (C, D) Histological sections of the bone defects obtained 5 weeks after implantationof ACS with 1.8×10^7 H1/fBMP-2 polyhedra. New bone (NB) formation was induced in ACS. Many polyhedra remained in the fibrous connective tissue. Arrows indicate polyhedra. Insert shown at high magnification. Photomicrograph of the bone defects at 15 weeks following implantation of ACS with H1/fBMP-2 polyhedra. (E) Newly generated bone was entirely replaced by trabecular bone with hematopoietic bone marrow 15 weeks after implantation.

compared to the other groups. The mean BV in bone defects from the 1.8×10^7 H1/fBMP-2 polyhedron group was significantly higher than that of the 3.6×10^6 H1/fBMP-2 polyhedron group (Fig. 6B).

Histological analysis showed that ACS and polyhedron cubes remained in the fibrous connective tissue in sections of tissue taken from implanted ACS that contained 1.8×10^7 H1/fBMP-2 polyhedra at 5 weeks after implantation. New bone was formed in ACS, but discontinuously from the edge of the host bone defect. However, at 15 weeks after implantation, histological analysis of the specimens revealed that the defects in which ACS containing 1.8×10^7 H1/fBMP-2 polyhedra had been implanted were filled with trabecular bone and that there was no evidence of any remnants of ACS or polyhedron cubes. Regenerated bone was integrated with the host bone at the defect margins and supported a robust bone marrow. A llamellar bone pattern was visible in the regenerated bone tissues (Fig. 6C-E). These findings suggest that newly generated bone establishes mature bone tissue. Additionally, there was no evidence of inflammatory or foreign-body reaction from the host tissues adjacent to the new bone. These results suggest that implants of ACS containing H1/fBMP-2 polyhedra induced new bone formation in a dose- and time-dependent manner.

Discussion

It is known that BMP-2 promotes bone healing and that ACS impregnated with rhBMP-2 supports long-term osteogenicity. But the complete healing of critical-sized bone defects cannot be induced by ACS with rhBMP-2, suggesting that a major problem remains to be solved in a drug delivery system (DDS) consisting of ACS.

In this study, we have shown that H1/fBMP-2 polyhedra enhance chondrogenic and osteogenic differentiation of progenitor ATDC5 cells. We also demonstrated that phosphorylation of endogenous Smad1/5 protein of ATDC5 cells was induced by H1/fBMP-2 polyhedra, indicating that the TGF-β and BMP signaling pathways are activated. These results suggest that H1/fBMP-2 polyhedra possess long-acting biological activity that enhances bone regeneration. In the no-implant and implant of ACS with empty polyhedra, bone repair did not proceed from the periosteum on the outer and inner surfaces near the bone defect. Conversely, ACS containing H1/fBMP-2 polyhedra induced near complete repair of critical-sized calvarial bone defects.

In current clinical practice, rhBMP-2 is soaked onto ACS for bone regeneration. However, complications associated with rapid protein degradation and diffusion, the cost of the high doses required for efficacy, and concerns over a correlation between extremely high doses of rhBMP-2 and cancer incidence suggest that spatiotemporal delivery strategies are necessary for the efficacy, efficiency, and safety of recombinant growth factor delivery[9,10,20–22]. Loading of the carriers through simple adsorption produces a quick release of biological activity that is considered unsuitable from a physiological point of view. Therefore, suitable carriers have the ability to provide controlled release of the rhBMP-2.

DDS has emerged as a promising method of efficiently applying medicines with short biological half-life. It is defined that DDS is a system that administers a drug by enhancing its absorption and prolonging its activity by sustaining delivery at a fixed rate over a set time period and precisely targeting a specific area within the body[23]. Collagen and gelatin have been used as biodegradable carriers for DDS for administration of rhBMP-2[24]. Since rhBMP-2 has a low

affinity to collagen, this approach requires the use of very high doses of rhBMP-2[6,7]. Visser and co-workers reported application of a genetically engineered BMP-2 fused to a collagen-binding domain in combination with ACS for the induction of ectopic bone formation[25]. It is known that the isoelectric point of gelatin can be easily changed by manipulating the conditions of preparation from collagen. Biodegradable gelatin hydrogels from alkaline gelatin that can ionically interact with acidic growth factors have the ability to control the release of rhBMP-2 and induce ectopic bone formation[26]. Thus, it is important to note that one of the most critical characteristics of DDS is its ability to maintain physiologic levels of rhBMP-2 within a limited space for a sufficient time to stimulate bone formation[21]. To date, despite the ready availability of rhBMP-2 for clinical use, there is no optimal DDS that can decrease the dose of rhBMP-2 and keep a more sustained release pattern and be effective for bone regeneration[21].

Under physiological conditions, polyhedral microcrystals are inert and insoluble[15,16]. These properties allowed us to employ these complexes as versatile micron-sized carriers of growth factors. We have demonstrated in this study that H1/fBMP-2 polyhedra efficiently stimulate differentiation of ATDC5 cells. Thus, polyhedra encapsulating BMP-2 with a H1 tag are micron-sized bioactive substances. Release of BMP-2 from polyhedral microcrystals occurs as a result of the decay of H1/fBMP-2 polyhedra by proteases secreted from surrounding cells. Although we have not determined the optimal therapeutic dose of H1/fBMP-2 polyhedra for this application, we estimated that 3.6×10^7 H1/fBMP-2 polyhedra contained the equivalent of 1 μg of BMP-2 protein. We found that 3.6×10^6 or 1.8×10^7 H1/fBMP-2 polyhedra enhanced bone regeneration compared to the rhBMP-2 group. Statistical analysis showed that 1.8×10^7 H1/fBMP-2 polyhedra had a stronger effect on bone regeneration than 3.6×10^6 H1/fBMP-2 polyhedra. It is therefore clear that there is a dose-dependent effect of BMP-2 delivered using this polyhedron delivery system.

It is important to design and improve delivery systems for growth factors. For many growth factors, their biological actions during physiologic events follow distinct patterns and only certain defined amounts of protein are released at predetermined times into the tissues. A slow-release system may be required because BMP-2 clearance might be faster than the bone-induction response of the host. In this study, histological examination showed polyhedron cubes were present in bone sections 10 weeks after implantation, but not at 15 weeks after implantation (Fig. 6C–E). These results suggest that polyhedron particles were absorbed and BMP-2 protein was secreted for 10 or more weeks. Further, we suggest that the effects of bone regeneration can be prolonged by immobilization of BMP-2 in polyhedron particles and we demonstrate a means by which such particles might be applied in clinical therapy.

The basic requirement for a delivery system is that it does not produce any unexpected inflammatory reactions due to cytotoxicity or immunogenicity when used in human therapy. Histological examination showed that there was no evidence of inflammatory cells from the host tissues adjacent to the polyhedral microcrystals. Collagen sponge has a long safety history as a hemostatic agent and wound-covering material[27,28]. Polyhedral microcrystals are resistant to desiccation and they can easily be contained in the atelocollagen sponge. Our data suggest that applying polyhedra using atelocollagen sponges may improve bone regeneration therapy. For these reasons, insect polyhedral microcrystals might provide a reliable growth factor delivery system, although further tests in large animals will be essential before it can proceed to the clinical setting.

Methods

Materials. BaculoGold™-linearized baculovirus DNA was purchased from BD Biosciences Pharmingen. Fetal bovine serum was purchased from Biological Industries for mammalian cell culture and BioWest for insect cell culture. Dulbecco's modified Eagle's/Ham's F12 medium (1:1), insulin and alcian blue solution were purchased from Wako pure chemical industries. Transferrin was from Roche Applied Sciences. Sodium Selinite and Alizarin red were from Sigma-Aldrich. Recombinant human BMP-2 (rhBMP-2) and anti-rhBMP-2 antibody were purchased from R&D systems. Absorbable atelocollagen sponge, Pelnac® was purchased from Gunze. All other chemicals and reagents were purchased from Nacalai Tesque.

Construction of BMP-2 polyhedra. The cDNA encoding the BMP-2 ORF was purchased from Toyobo in an entry vector and subcloned into each destination vector (pDEST/VP3-S(N), pDEST/VP3-S(C), pDEST/VP3-L and pDEST/H1) using LR clonase according to the manufacturer's directions. Four types of transfer vector were produced: pTransVP3-S(N)/full-length BMP-2, pTransVP3-S(C)/full-length BMP-2, pTransVP3-L/full-length BMP-2 and pTransH1/full-length BMP-2.

For subcloning of the BMP-2 gene encoding the pro-form (proBMP-2, 24-396 amino acids) or the mature form (mBMP-2, 293-396 amino acids), DNA fragments were amplified by PCR using different primer combinations: forward primers were 5′-GGGGACAAGTTTGTACAAAAAAGCAGGCTCCATGCAAGCCAAACACAAACAGCGGA-3′, 5′-GGGGACAAGTTTGTACAAAAAAGCAGGCTCCCAAGCCAAACACAAACAGCGGAAAC-3′ and 5′-GGGGACAAGTTTGTACAAAAAAGCAGGCTCCCTCGTTCCGGAGCTGGGC-3′, and reverse primers were 5′-GGGGACCACTTTGTACAAGAAAGCTGGGTAGCGACACCCACAACCCTCCACAACC-3′ and 5′-GGGGACCACTTTGTACAAGAAAGCTGGGTACTAGCGACACCCACAACCCTCCACAACC-3′. attB-flanked PCR products were then inserted into the donor vector (pDONR221) using a BP clonase reaction. Each BMP-2 gene, cloned between attL1 and attL2 sites in the entry vector, were transferred to destination vectors via LR clonase reactions resulting in production of the transfer vectors encoding the mature or the pro-form of BMP-2 fused with VP3 or H1 tags (pTransVP3-S(N)/pro-form BMP-2, pTransVP3-L/pro-form BMP-2, pTransH1/pro-form BMP-2, pTransVP3-S(C)/mature BMP-2, pTransVP3-L/mature BMP and pTransH1/mature BMP-2). These transfer vectors were co-transfected into Sf21 insect cells with BaculoGold™ baculovirus linearized DNA. After incubation for 5 days at 27°C, recombinant baculoviruses expressing the full-length, pro-form, and mature forms of BMP-2 with VP3 or H1 tags were harvested and stored at 4°C.

Purification of polyhedra immobilized with BMP-2 proteins. To generate empty (CP-H) polyhedra, *Spodoptera frugiperda* IPLB-SF21-AE cells (Sf cells) were inoculated with recombinant baculovirus AcCP-H29/PDI expressing BmCPV polyhedrin and PDI, in which BmCPV polyhedrin and PDI were expressed under the control of the baculovirus polyhedrin promoter and p10 promoter, respectively. For production of BMP-2 polyhedra, Sf cells were co-infected with AcCP-H29/PDI and another recombinant baculovirus expressing recombinant BMP-2 fused with the VP3 or H1 tags. The infected cells were cultured for 10 days at 27°C and then the cells were harvested in a conical tube by centrifugation. The cell pellet was resuspended in phosphate-buffered saline (PBS; pH 7.2) and treated with an ultrasonic homogenizer at 6% power for 30 sec. The cell homogenate was centrifuged at 1500 × g at 4°C and the supernatant was removed. These treatments were repeated and the purification was complete. The polyhedron suspension was adjusted to the same density (5×10^4 cubes per microliter volume) and stored at 4°C in distilled water containing 100 units/ml penicillin and 100 μg/ml streptomycin.

Cell culture. ATDC5 cells were maintained in culture medium containing DME/Ham's F12 (1:1) medium with 10 μg/ml insulin, 10 μg/ml transferrin, 3.2×10^{-8} M sodium selenite, 5% fetal bovine serum, 100 units/ml penicillin and 100 μg/ml streptomycin at 37°C in humidified air with 5% CO_2. To test the biological activity of each BMP-2 polyhedra construct, polyhedra were spotted and desiccated on the bottom of wells of a culture plate (Iwaki). The seeding density of the cells was 3×10^3 cells/well in a 96-well culture plate, 2×10^4 cells/well in a 24-well culture plate and 1×10^6 cells/well in a 6-well culture plate. For assay of release of BMP-2, polyhedra were spotted and desiccated on a 0.4 μm pore size membrane cell culture insert (BD Biosciences). Cells were then seeded in each well of the cell culture plate.

Chondrogenic and osteogenic differentiation of ATDC5 cells. After cultivation, cells were washed with PBS, fixed with methanol for 20 min and incubated with alcian blue solution for 16 hours at room temperature. After washing with water, cell images were captured. In addition, stained cells were lysed with 6 M guanidine hydrochloride solution and the absorbance of lysates was measured at 620 nm. For detection of mineralization, cells were cultured for 15 days or 28 days and fixed in methanol for 20 min. Cells were then stained with alizarin red solution for 16 hours at room temperature. Images were obtained by scanning the plate on a flat-bed scanner.

Assay of phosphorylation of Smad1/5. For measurement of phosphorylated Smad1/5 in ATDC5 cells, confluent cultivated cells were stimulated with BMP-2 polyhedra or rhBMP-2 suspended in the culture medium and incubated for several time points at 37°C under 5% CO_2 in air. The stimulated cells were rinsed with ice-cold PBS and lysed in SDS-PAGE sample buffer. All samples were resolved by 12.5% SDS-PAGE and transferred to a nitrocellulose membrane at 1 mA/cm^2 for 90 min. The membranes were treated with primary antibody (anti-phosphorylated Smad1/5 antibody or anti-Smad1/5 antibody) with a 1:1000 dilution. After washing three times, the membrane was incubated with a 1:3000 dilution of goat anti-mouse IgG conjugated to horseradish peroxidase (BioRad) for 2 hours at room temperature.

Results were visualized by Chemilumi-One (Nacalai Tesque) and captured using an image scanner.

Preparation of ACS impregnated with BMP-2 polyhedra or rhBMP-2. We estimated that the average mass of BMP-2 immobilized in a polyhedral microcrystal was $\sim 2.8 \times 10^{-5}$ ng (the average volume of a microcrystal is $5 \times 5 \times 5$ μm^3). Hence, 3.6×10^7 polyhedral microcrystals contained approximately 1 μg of recombinant protein. We mixed 1.8×10^7 or 3.6×10^6 H1/fBMP-2 polyhedra with 50 μl PBS and incorporated them into an absorbable atelocollagen sponge by air-drying for 12 hours at room temperature. The ACS was cut into columns (diameter: 9 mm, height: 1 mm) and used for retention of polyhedral microcrystals and as a scaffold for bone regeneration. An ACS containing 1.8×10^7 or 3.6×10^6 CP-H polyhedra served as the empty polyhedra. A 50 μl aliquot of rhBMP-2 (Yamanouchi Pharmaceutical) solution prepared with 5 μg or 1 μg in PBS was dropped onto the sponge and left for 12 hours at 4°C to make the rhBMP-2 ACS.

Animal study. All rats were maintained at Kanagawa Dental College under strict pathogen-free conditions and animal experiments were approved by the animal-study guidelines of the college.

Surgical procedure. To study *in vivo* bone regeneration, we produced calvaria bone defects in 84 skeletally mature, 18-week-old, male Wistar rats weighing 350–400 g (Japan SLC). We sedated rats with an intraperitoneal injection of pentobarbital. A semilunar incision was then made in the scalp in the anterior region of the calvarium, allowing reflection of a full-thickness flap in the posterior direction. We prepared a 9 mm-diameter bone defect in the calvaria bone with a trephine bur (Technica) copiously irrigated with sterile saline water.

The 84 rats were divided into seven experimental groups consisting of 12 rats in each group. High-quantity polyhedron group, 1.8×10^7 polyhedral microcrystals of H1/fBMP-2 polyhedra; low-quantity polyhedron group, 3.6×10^6 polyhedral microcrystals of H1/fBMP-2 polyhedra; high quantity rhBMP-2 solution group, 5 μg of rhBMP-2; low quantity rhBMP-2 solution, 1 μg of rhBMP-2; empty polyhedron group, 1.8×10^7 or 3.6×10^6 polyhedral microcrystals of CP-H polyhedra; control group; no implant. The rats in each group were further divided into three groups (4 rats/group) depending on the duration of the experiment (5, 10 and 15 weeks). After creating the defects and implanting the experimental ACS, the soft tissues were then repositioned and sutured with 4-0 nylon monofilament to achieve primary closure (Fig. 1B–E).

Assessing bone regeneration. To assess bone regeneration, we sacrificed rats with a lethal intravenous dose of pentobarbital after implantation. The area of the original surgical bone defect and surrounding tissues was removed *en bloc* and fixed in a 10% solution of neutral-buffered formalin. We produced images of all regions surrounding the calvaria bone defects by soft-X-ray radiography (Sofron Type SRO-M50, Soken) using electroscopic film (Fuji Photo Film). All images included a hydroxyapatite (HAp) step-wedge in order to correct for unequally developed film. We analyzed the soft-X-ray images with a program that analyses digital images (HC-2500/OL; WinROOF; Mitani) to determine BMC. The center of regenerated bone in the bone defect in each group was encircled by a closed line and the measurement area was specified. Blackening was measured in the area and the amount of HAp corresponding to this value was calculated.

μ-CT 3D reconstruction. Tissue specimens were scanned by μ-CT on a Scan Xmate-L090 (Comscan). Reconstructed images were analyzed with 3D-BON software (Ratoc System Engineering). Circular regions of 9 mm in diameter were cropped as the region of interest (ROI). BV was then evaluated in the ROI.

Histological procedures and analysis. Tissue specimens were fixed in 10% formalin, decalcified in 22.5% formic-acid solution, dehydrated with ethanol, and embedded in paraffin. We histologically observed 6 μm thin-sections stained with hematoxylin and eosin using an optical microscope (Olympus).

1. Reddi, A. H. Symbiosis of biotechnology and biomaterials: applications in tissue engineering of bone and cartilage. *J Cell Biochem* **56**, 192–195 (1994).
2. Reddi, A. H. BMPs: actions in flesh and bone. *Nat Med* **3**, 837–839 (1997).
3. Schmitt, J. M, Hwang, K., Winn, S. R. & Hollinger, J. O. Bone morphogenetic proteins: an update on basic biology and clinical relevance. *J Orthop Res* **17**, 269–278 (1999).
4. Zabka, A. G. *et al.* Histomorphometric description of allograft bone remodeling and union in a canine segmental femoral defect model: a comparison of rhBMP-2, cancellous bone graft, and absorbable collagen sponge. *J Orthop Res* **19**, 318–327 (2001).
5. Liu, Y., Hunziker, E. B., Layrolle, P., De Bruijn, J. D. & De Groot, K. Bone morphogenetic protein 2 incorporated into biomimetic coatings retains its biological activity. *Tissue Eng* **10**, 101–108 (2004).
6. Geige, r M., Li, R. H. & Friess, W. Collagen sponges for bone regeneration with rhBMP-2. *Adv Drug Deliv Rev* **55**, 1613–1629 (2003).
7. Swiontkowski, M. F. *et al.* Recombinant human bone morphogenetic protein-2 in open tibial fractures. A subgroup analysis of data combined from two prospective randomized studies. *J Bone Joint Surg Am* **88**, 1258–1265 (2006).
8. Zhao, B. *et al.* Heparin potentiates the in vivo ectopic bone formation induced by bone morphogenetic protein-2. *J Biol Chem* **281**, 23246–23253 (2006).
9. Govender, S. *et al.* Recombinant human bone morphogenetic protein-2 for treatment of open tibial fractures: a prospective, controlled, randomized study of four hundred and fifty patients. *J Bone Joint Surg Am* **84-A**, 2123–2134 (2002).
10. McKay, W. F., Peckham, S. M. & Badura, J. M. A comprehensive clinical review of recombinant human bone morphogenetic protein-2 (INFUSE Bone Graft). *Int Orthop* **31**, 729–734 (2007).
11. Cahill, K. S., Chi, J. H., Day, A. & Claus, E. B. Prevalence, complications, and hospital charges associated with use of bone-morphogenetic proteins in spinal fusion procedures. *JAMA* **302**, 58–66 (2009).
12. Benglis, D., Wang, M. Y. & Levi, A. D. A comprehensive review of the safety profile of bone morphogenetic protein in spine surgery. *Neurosurgery* **62**, ONS423–431; discussion ONS431 (2008).
13. Paramore, C. G. *et al.* The safety of OP-1 for lumbar fusion with decompression--a canine study. *Neurosurgery* **44**, 1151–1155; discussion 1155–1156 (1999).
14. Lo, K. W., Ulery, B. D., Ashe, K. M. & Laurencin, C. T. Studies of bone morphogenetic protein based surgical repair. *Adv Drug Deliv Rev* (2012).
15. Rohrmann, G. F. Polyhedrin structure. *J Gen Virol* **67**, 1499–1513 (1986).
16. Mori, H. & Metcalf, P. Cypoviruses. *Insect Virology*, ed Asgari S., Johnson, K. N. (Caister Academic Press), pp 307–324 (2010).
17. Coulibaly, F. *et al.* The molecular organization of cypovirus polyhedra. *Nature* **446**, 97–101 (2007).
18. Mori, H. *et al.* Expression of Bombyx mori cytoplasmic polyhedrosis virus polyhedrin in insect cells by using a baculovirus expression vector, and its assembly into polyhedra. *J Gen Virol* **74**, 99–102 (1993).
19. Ijiri, H. *et al.* Structure-based targeting of bioactive proteins into cypovirus polyhedra and application to immobilized cytokines for mammalian cell culture. *Biomaterials* **30**, 4297–4308 (2009).
20. Seeherman, H. & Wozney, J. M. Delivery of bone morphogenetic proteins for orthopedic tissue regeneration. *Cytokine Growth Factor Rev* **16**, 329–345 (2005).
21. Meikle, M. C. On the transplantation, regeneration and induction of bone: the path to bone morphogenetic proteins and other skeletal growth factors. *Surgeon* **5**, 232–243 (2007).
22. Boyne, P. J. *et al.* A feasibility study evaluating rhBMP-2/absorbable collagen sponge for maxillary sinus floor augmentation. *Int J Periodontics Restorative Dent* **17**, 11–25 (1997).
23. Tsuzuki, N. *et al.* In vivo osteoinductivity of gelatin beta-tri-calcium phosphate sponge and bone morphogenetic protein-2 on an equine third metacarpal bone defect. *Res Vet Sci* **93**, 1021–1025 (2012).
24. Takahashi, Y., Yamamoto, M., Yamada, K., Kawakami, O. & Tabata, Y. Skull bone regeneration in nonhuman primates by controlled release of bone morphogenetic protein-2 from a biodegradable hydrogel. *Tissue Eng* **13**, 293–300 (2007).
25. Visser, R., Arrabal, P. M., Becerra, J., Rinas, U. & Cifuentes, M. The effect of an rhBMP-2 absorbable collagen sponge-targeted system on bone formation in vivo. *Biomaterials* **30**, 2032–2037 (2009).
26. Yamamoto, M., Takahashi, Y. & Tabata, Y. Controlled release by biodegradable hydrogels enhances the ectopic bone formation of bone morphogenetic protein. *Biomaterials* **24**, 4375–4383 (2003).
27. Chvapil, M. Collagen sponge: theory and practice of medical applications. *J Biomed Mater Res* **11**, 721–741 (1977).
28. Friess, W., Lee, G. & Groves, M. J. Insoluble collagen matrices for prolonged delivery of proteins. *Pharm Dev Technol* **1**, 185–193 (1996).

Acknowledgments

This work was supported in part by A-STEP exploratory research AS232Z00847F from JST and Grants-in-Aid for Scientific Research (A) 22241052 and (C) 90237131 from JSPS.

Author contributions

G.M., S.K. and H. Mori designed and performed research. T.U., H.I., S.J., D.G.A. and E.K. provided materials. J.S., Y.O., H.Y., Y.S., K.K., H. Maeda, Y.K. and G.M. interpreted data. G.M. and H. Mori wrote the paper.

Additional information

Supplementary Information accompanies this paper at http://www.nature.com/scientificreports

Competing financial interests: The authors declare no competing financial interests.

How to cite this article: Matsumoto, G. *et al.* Bone regeneration by polyhedral microcrystals from silkworm virus. *Sci. Rep.* **2**, 935; DOI:10.1038/srep00935 (2012).